

ANGLE-RESOLVED X-RAY PHOTOELECTRON SPECTROSCOPY STUDY OF THE THIOUREA DERIVATIVE ADSORPTION ON Au(111) FROM ETHANOLIC SOLUTION

ESTUDIO DE LA ADSORCIÓN SOBRE Au(111) DE UN DERIVADO DE TIOUREA EN DISOLUCIÓN ETANÓLICA MEDIANTE ESPECTROSCOPIA DE ELECTRONES

M.P. HERNÁNDEZ^{at}, G. NAVARRO-MARÍN^a, O. ESTÉVEZ-HERNÁNDEZ^a, M.H. FARIAS SÁNCHEZ^b

a) Instituto de Ciencia y Tecnología de Materiales (IMRE), Universidad de La Habana, Zapata y G, El Vedado, Plaza de la Revolución, La Habana 10400, Cuba; mayrap@imre.uh.cu[†]

b) Centro de Nanociencias y Nanotecnología (CNYN), Universidad de Nacional Autónoma de México (UNAM), km 107 Carretera Tijuana-Ensenada, Ensenada, Baja California, 22860, México

[†] corresponding author

Recibido 20/3/2017; Aceptado 21/7/2017

The adsorption of 1-(2-Furoyl)-3-[3-(trifluoromethyl)phenyl] thiourea on Au(111) from ethanolic solution, was studied by means of angle-resolved X-ray photoelectron spectroscopy (AR-XPS). The AR-XPS spectra were obtained at different take-off angles with respect to substrate surface: (50°, 70°, 90° and 110°). The spectra of the C1s at different take-off angles indicated the degradation of CF₃ species towards CF₂ and CF entities. This degradation is due to damages provoked for the effect of the electrons induced by X-ray excitation. High resolution spectra of F1s at these angles, showed two peaks at 687.6 and 688.4 eV, confirming the presence of the organic fluorine (C-F) and inorganic fluoride (F⁻). The X-ray-photoelectron angular measurements were capable of yielding thickness-to-mean free path ratios for the adsorbed layer. Despite of the fluorine lost, such measurements demonstrate the permanence of the CF₃ groups in the *meta*-phenyl position at 10 ± 1 Å of the inorganic fluoride. A preferential orientation of the species (CF_{x=1,2,3}) at 50° respect to the surface of the substrate was observed.

La adsorción de 1-(2-Furoil)-3-[3-(trifluorometil)fenil]tiourea sobre Au(111) en una disolución etanólica, se estudió mediante la distribución angular de fotoelectrones de rayos X (AR-XPS). Los espectros de AR-XPS se obtuvieron a diferentes ángulos de detección con respecto a la superficie del sustrato: 50°, 70°, 90° y 110°. En los espectros angulares de C1s se observa la degradación del grupo CF₃ en las especies CF₂ y CF. Esta degradación es provocada por el efecto de los electrones inducidos por la excitación de los rayos X. Los espectros de alta resolución de F1s en estos ángulos, mostraron dos picos a 687,6 y 688,4 eV, confirmando la presencia de flúor orgánico (C-F) y flúor inorgánico (F⁻). Las mediciones angulares de fotoelectrones permitieron determinar la relación entre el espesor de la capa de moléculas y el recorrido libre medio de los electrones en la capa adsorbida. A pesar de las pérdidas de flúor, tales mediciones demostraron que los grupos CF₃ permanecen en la posición *meta* del anillo bencénico a una distancia 10 ± 1 Å del flúor inorgánico. Las especies (CF_{x=1,2,3}) mostraron una orientación preferencial a 50° respecto a la superficie del sustrato.

PACS: Auger spectroscopy, 82.80.Pv; Electron beam radiation effects, 61.80.Fe; Physisorption, 68.43.-h

Clarifying the nature of interactions between metal electrodes and organic molecules still represents one of the challenging problems in molecular electronics that needs to be solved in order to optimize electron transport through a molecular device.

Photoemission is an ideal technique to provide information about the electronic structure of surfaces [1–3]. X-ray photoelectron spectroscopy (XPS) determines the elemental composition of a surface, including quantification and also with chemical bonding information. Another utilization of XPS is to analyze separately parts from a single molecule, in order to discriminate them. XPS has this potential because of its nanometric probing depth. This capability is used to find a certain functional group of interest in a molecule specifically appearing on the outermost surface and giving it special kinds of properties. The angular distribution of photoelectrons is used to understand the relation between the functionality of the surface structure and the transfer property of a particular single molecule. One also can

determine the absolute value of the photoelectron mean free path.

Thiourea derivatives are versatile compounds with several electronic centers. The reports about adsorption on gold surface of this kind of molecules is scarce. Previous studies have been focused mainly on simple thiourea using Voltammetry and Electrochemical Scanning Tunneling Microscopy (EC-STM). We here report the adsorption of the thiourea derivative 1-(2-Furoyl)-3-[3-(trifluoromethyl)phenyl]thiourea on Au(111). It was studied by means of XPS. This molecule contains a 2-furoyl group on one side of the thiourea moiety and a 3-monosubstituted phenyl group on the other side. The electronic properties of these compounds can be affected by the type of substituent and its position, resulting in the variation of the spatial configurations, which have important effects on the electronic properties. The investigation of the electronic properties of this molecular-metal junction may lead to the development of new molecular systems composed

by these single-molecules with application in heavy metal sensors.

This paper demonstrates the degradation of the CF₃ substituent to CF₂ and CF species by monitoring spectral changes on the C 1s transition from 1-(2-Furoyl)-3-[3-(trifluoromethyl)phenyl]thiourea molecule (C₁₃H₉F₃N₂O₂S) (Figure 1). Additionally, the angular distribution of the photoelectrons of the F1s made possible to determine the distance between C-F and F⁻ entities.

I. EXPERIMENTAL DETAILS

I.1. C₁₃H₉F₃N₂O₂S synthesis

The C₁₃H₉F₃N₂O₂S molecule was prepared according to a previous procedure by Otazo et al [4]. Gold substrates were supplied by Arrandee.

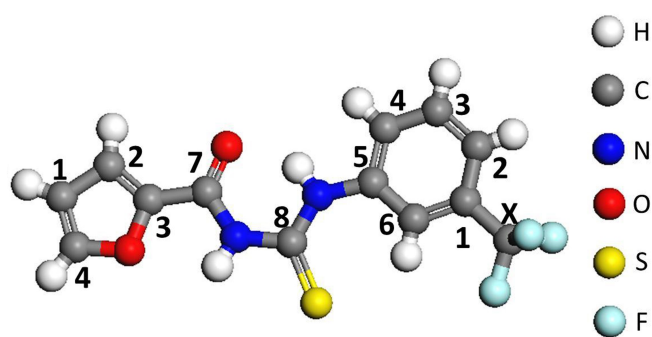


Figure 1. Scheme of the C₁₃H₉F₃N₂O₂S molecule.

I.2. Preparation of the C₁₃H₉F₃N₂O₂S molecule on Au(111)

50 mg of the C₁₃H₉F₃N₂O₂S molecule were dissolved in 5 ml of ethanol. The gold substrate was annealed in butane flame for 3 min to produce flat terraces with a (111) preferred orientation. The substrate was immersed in the ethanolic solution during 24 h at room temperature. Later, it was rinsed with abundant deionized water and dried under a N₂ stream.

I.3. Spectroscopic analysis

XPS and AR-XPS spectra were collected on a SPECS custom-made system using a PHOIBOS 150 WAL hemispherical analyzer and a monochromatized Al K_α line (1486.6 eV) from μ-FOCUS 500 x-ray monochromator. A two-point calibration of the energy scale was performed by using gold (Au 4f_{7/2}), binding energy at 84.0 eV and copper (Cu 2p_{3/2}), binding energy at 932.7 eV. Au 4f_{7/2} at 84.0 eV was used as the energy reference in order to subtract charging shifts. Shirley-type background was subtracted from each high resolution spectrum. The best fit with the experimental values was a combination of Gaussian/Lorentzian functions (Gaussian/Lorentzian ratio of 70/30). Measurements were

performed at different take-off angles (θ = 50°, 70°, 90° and 110°) with respect to surface.

II. ANALYSIS PROCEDURE

The photoelectron intensity from a thin film-covered substrate varies with the take-off angle, θ, as given by [5]

$$\ln(I) = -\frac{d}{\lambda \sin(\theta)} + \ln(I_0), \quad (1)$$

where I₀ and I are the intensities of the photoelectrons from clean substrate and from substrate covered with a thin film of thickness d, respectively, and λ is the photoelectron mean free path. According to (1), ln(I) should be linearly related to 1/(sinθ) with the slope of -(d/λ). Kondo et al. proposed the following equation to calculate d (in Å) for organic thin films [6]

$$-\frac{d}{\lambda} = d \frac{E_p^2}{E_k} \left[\beta \ln\left(0.191 \frac{E_k}{\rho(d)^{0.5}}\right) - \frac{1634 - 0.91E_p}{829.4E_k} + \frac{4429 - 20.8E_p}{829.4E_k^2} \right] \quad (2)$$

where E_k (eV) is the kinetic energy of the photoelectron, E_p (eV) is the free electron plasmon energy and β is an empirical parameter. E_p and β are given by following two equations:

$$E_p = 28.8 \sqrt{\frac{N_v \rho(d)}{M}}, \quad (3)$$

$$\beta = -0.10 + 0.944(E_p^2 + E_g^2)^{-0.5} + 0.069 \rho(d)^{0.1}, \quad (4)$$

being M, N_v and E_g the molecular weight, the number of valence electrons of the overlayer molecule and the edge energy of the optical absorption, respectively.

In the case of a monolayer formed by adsorbed molecules on surface, ρ(d) can be used as:

$$\rho(d) = \frac{\Gamma M}{N_A d}, \quad (5)$$

where Γ is the adsorbed amount of molecules on the substrate (molecules cm⁻²) and N_A is Avogadro's number.

Taking into account these equations, (d/λ) can be determined from the AR-XPS measurement, the slope of the plot of ln(I) versus 1/(sinθ), as shown in (1), and Γ can be electrochemically determined by measuring the charge of the reductive desorption in a basic solution [7], then, d will be solution of equation (2).

III. DISCUSSION

Figure 2 presents the S 2p XPS spectra. It shows a broad peak with pronounced asymmetry toward larger binding energies. The solid line in Figure 2 is the best fit to the cumulative spectrum with two species. The sulfur species obtained by this fit were S 2p_{3/2} with binding energies at 161.8 ± 0.2 and 163.6 ± 0.2 eV. The S 2p binding energies

of sulfur are characteristic of the molecular structure and are predominantly determined by the electronegativities of nearest-neighbor atoms. The lower binding energy at 161.8 eV corresponds to thiourea adsorbed. It is assigned by comparing with previously published S 2*p* reference peaks [8]. In the case of the minority sulfur species at 163.6 eV, various assignments are possible i.e., sulfur adsorbed either as multilayers and/or thioureas multilayers.

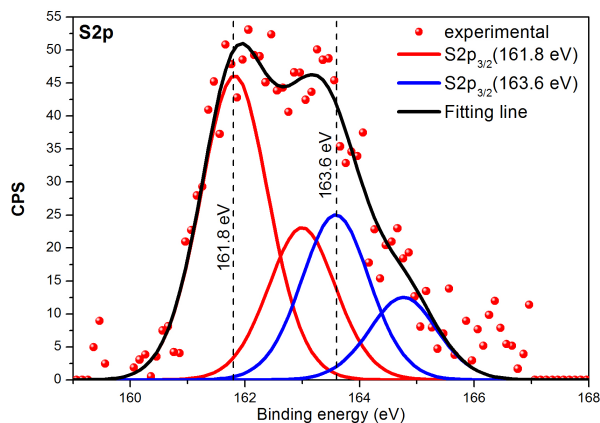


Figure 2. S 2*p* spectra of $C_{13}H_9F_3N_2O_2S$ at high intensity mode (HIM).

Figures 3 and 4 show C 1*s* and F 1*s* spectra of the $C_{13}H_9F_3N_2O_2S$ on Au(111) detected at various angles θ . The C 1*s* spectra can be deconvoluted into component 1 at 284.6 eV (C-C for hydrocarbon and $C_{i,i=1,2}$ for furoyl), component 2 at 285.6 eV ($C_{i,i=3,4,5}$ for phenyl), component 3 at 286.9 eV ($C_{i,i=1,2,6}$ for phenyl and $C_{i,i=3,4}$ for furoyl), component 4 at 287.8 eV (C=O), component 5 at 289.3 eV (C-F), component 6 at 291.3 eV ($-CF_2$) and component 7 at 292.9 eV ($-CF_3$). The F 1*s* components 1 at 687.4 eV (F^-) and 2 at 688.4 eV (C-F) were determined by peak component fitting. The (F^-) ion is expected to be adsorbed on gold. F 1*s* and C 1*s* binding energies (eV) are summarized in Table 1.

Table 1. C 1*s* and F 1*s* binding energies (BE) in eV for $C_{13}H_9F_3N_2O_2S$ on Au(111).

C _{1s}	BE(eV)		Reference
	this work	reported	
C-C	284.6	284.6	[9]
C _{1fu} *, C _{2fu}		284.8	[10]
C _{4ph} **	285.6	285.5	[11]
C _{3ph} , C _{5ph}		286.0	
C _{2ph} , C _{6ph}	286.9	286.5	[11]
C _{3fu} , C _{4fu}		286.6	[10]
C _{1ph}		286.9	[11]
C ₇	287.8	287.7	[12]
> C = S		288.1	[13]
X=CF	289.3	288.9	[14]
X=CF ₂	291.3	291.3	[14]
X=CF ₃	292.9	292.9	[14]
F _{1s}			
C-F	688.4	688.8	[14]
Au-F	687.4	687.6	[15]

*fu=furoyl
**ph=phenyl

The intensities of F 1*s* peaks have a maximum value at 70° and decrease slightly in the remaining take-off angles. The

decreasing of the C 1*s* intensities with θ is associated with asymmetric distribution of the carbon atoms. Figure 1 shows that furoyl group is on one side of the thiouride core and phenyl group is on the other side.

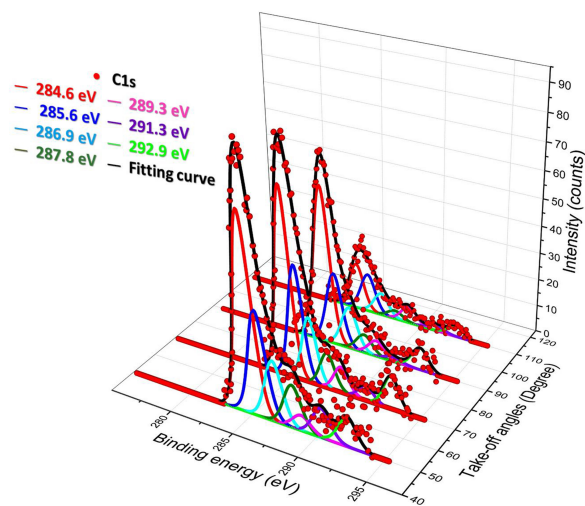


Figure 3. C 1*s* AR-XPS spectra of $C_{13}H_9F_3N_2O_2S$ at different emission angles.

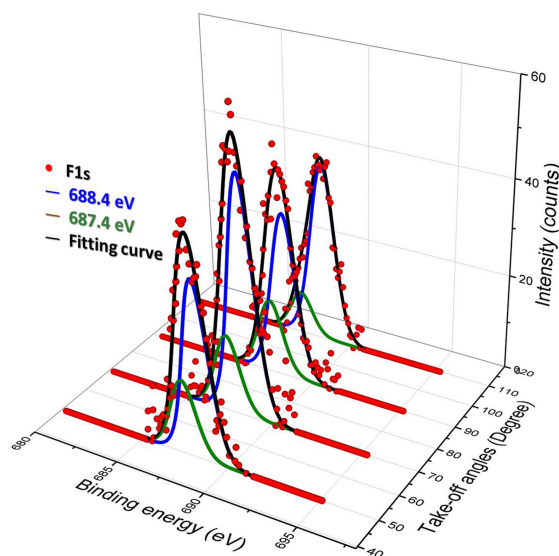


Figure 4. F 1*s* AR-XPS spectra of $C_{13}H_9F_3N_2O_2S$ at different emission angles.

By applying equations (2)-(5) to F 1*s* spectra, we can estimate the distance between organic fluorine (CF_i $i=1,2,3$) and inorganic fluoride adsorbed on gold (Au-F). The values employed in the calculation were as follows: $-d_{organic\ fluorine}/\lambda = -4.9$ and $-d_{inorganic\ fluoride}/\lambda = -5.2$, obtained as the slope of the $\ln(I)$ versus $\sin(\theta)^{-1}$, $\Gamma = 1.25 \cdot 10^{15}$ molecules cm^{-2} [16], $M=314$ g mol^{-1} ($C_{13}H_9F_3N_2O_2S$), $N_v=117$ ($C=13, H=9, F=3, N=2, O=2$) and $E_g=4.75$ eV [17], which is edge energy in the absorption spectra of benzene [14]. The $E_K=798.2$ eV for C-F and $E_K=799$ eV for (F^-), were calculated by subtracting the binding energy of the F 1*s* for organic fluorine (688.4 eV) and inorganic fluoride (687.6 eV) from incident X-ray energy of 1486.6 eV. The chosen E_g value for benzene may lead to some error, since the surface layer

consists not only of the benzene group. However, this error must be small because the value of E_g does not affect β value significantly, due to E_p is larger than E_g (see (2),(4)). The value of the $d_{\text{organic fluorine}} - d_{\text{inorganic fluoride}}$ is $\approx 10 \pm 1 \text{ \AA}$ and $\lambda=30 \pm 1 \text{ \AA}$ for both, C-F and F^- entities.

The fluorocarbon species are associated with phenyl group, thus the distance between these groups and the substrate surface determines the relative position of the phenyl group in the molecule. An evaluation of the electrical properties in that spatial configuration will allow to be able to select a new design based on the substituent position in the phenyl ring.

The molecular geometry could be described comparing the relative peak areas of the C 1s and F 1s of the fluorocarbon species (CF_x groups) at different take-off angles (see Table 1). For this, we employ the amount of fluorine at 688.7 eV and the sum of the C1, C2 and C3 at 289.3, 291.3 and 292.9 eV, respectively. The sensitivity factors for individual elements depend on the sampling depths, which in turn vary with the kinetic energies of the core level electrons. Bearing this in mind, we compared the intensities of carbon and fluorine atoms, considering that the sensitivity factors are approximately the same for all angles. Table 2 summarizes the relative peak area ratios between the carbons and fluorine of the fluorocarbon species with the take-off angles. The quantification of spectra obtained at take-off angles of 70, 90, 110° showed a similar ratio between the components, however at 50° the relative amount of carbon increased slightly. Therefore, the only plausible reason for the increased carbon signal from the surface layer (Table 2) is a preferential orientation of the fluorocarbon species (CF_x groups) from the closer take-off angle to surface. Although we do not know exactly the distance of the bond sulfur-gold to the fluorocarbon species, an estimated length, taking into account the bonding distances, is close to 13 Å. This fact along with a take-off angle of 50° allows us to determinate a fluorocarbon distance to the surface of 10 Å. This value is similar to that obtained for the distance between organic and inorganic fluoride confirming that at 50° the fluorocarbon species have a preferential orientation.

Table 2. Experimental C/F areas ratio at different take-off angles for $C_{13}H_9F_3N_2O_2S$ on Au(111).

take-off angles (deg)	$A_{C1} + A_{C2} + A_{C3}$ (counts·eV)	A_F (counts·eV)	Relative areas
50	47.8	67.5	0.708
70	33.6	91.5	0.367
90	23.5	64.0	0.367
110	20.7	70.0	0.296
A* = peak area			

IV. CONCLUSIONS

Chemical changes produced from the electrons induced by X-ray excitation include the partial transformation of CF_3 group by loss of fluorine towards CF_2 and CF species. The component of F 1s at 687.4 eV corresponds to inorganic fluoride, which must be assigned to fluorine adsorbed on Au(111). The distance between organic fluorine ($CF_{1,2,3}$ -meta-phenyl position) and the F atoms

of Au-F is $10 \pm 1 \text{ \AA}$. The AR-XPS measurements permit a characterization of the specimen geometric parameters and surface compositions. Both spatial configuration and position of substituents modulate the electronic properties of the molecule-substrate system.

ACKNOWLEDGEMENTS

MPH acknowledges DGAPA-UNAM for a 3-month fellowship through the "Programa de Estancias de Investigación en la UNAM (PREI)". The authors thank to David Domínguez for valuable AR-XPS measurements. This study was partially supported by the Basic Science National Project (PNCB) Code: PNCB-49-UH-15.

REFERENCES

- [1] G. Mette, D. Sutter, Y. Gurdal, S. Schnidrig, B. Probst, M. Iannuzzi, J. Hutter, R. Alberto and J. Osterwalder, *Nanoscale* **8**, 7958 (2016).
- [2] T. Fischer, P. M. Dietrich, C. Streeck, S. Ray, . Nutsch, A. Shard, B. Beckhoff, W. E. S. Unger, K. Rurack, Silane Monolayers on Surfaces via a Dual-Mode Fluorescence and XPS Label. *Anal. Chem.*, **87** 2685 (2015).
- [3] M. Nolan, S. D. Elliott, J. S. Mulley, R. A. Bennett, M. Basham and P. Mulheran, *Phys. Rev. B* **77**, 235424 (2008).
- [4] E. Otazo-Sánchez, P. Ortiz-del-Toro, O. Estevez-Hernández, Pérez-Marín, I. Goicochea, A. Cerón-Beltrán and J.R. Villagomez-Ibarra, *Spectrochim. Acta A* **58**, 2281 (2002).
- [5] C. S. Fadley, R. J. Baird, W. Siekhaus, T. Novakov and S. A. L. Bergstrom, *J. Electron Spectrosc.* **4**, 93 (1974).
- [6] T. Kondo, M. Yanagida, K. Shimazu and K. Uosaki, *Langmuir* **14**, 5656 (1998).
- [7] C. A. Widrig, C. Chung and M. D. Porter, *J. Electroanal. Chem.* **310**, 335 (1991).
- [8] O. Azzaroni, G. Andreasen, B. Blum, R. C. Salvarezza and A. J. Arvia, *J. Phys. Chem. B* **104**, 1395 (2000).
- [9] J. F. Moulder and W. F. Stickle, *Handbook X-Ray Photoelectron Spectroscopy*, 2nd Ed. (Physical Electronics Division, Perkin-Elmer Corporation, 1992), p. 41.
- [10] J. L. Solomon, R. J. Madix and J. Stöhr, *J. Chem. Phys.* **94**, 4012 (1991).
- [11] D. T. Clark, D. Killcast and W. K. R. Musgrave, *J. Chem. Soc. Chem. Comm.* **1**, 9 (1971).
- [12] D. Briggs and G. Beamson, *Anal. Chem.* **64**, 1729 (1992).
- [13] R. Srinivasan and R.A. Walton, *Inorg. Chim. Acta* **25**, L85 (1977).
- [14] F. Y. Zhang, S. G. Advani, A. K. Prasad, M. E. Boggs, S. P. Sullivan and T. P. Beebe, *Electrochim. Acta* **54**, 4025 (2009).
- [15] A. Szwajca, M. Krzywiecki and H. Koroniak, *J. Fluorine Chem.* **180**, 248 (2015).
- [16] A.E. Bolzan, R.C.V. Piatti, R.C. Salvarezza and A.J. Arvia, *J. Appl. Electrochem.* **32**, 611 (2002).
- [17] S. L. Murov and I. Carmichael, *Handbook of Photochemistry*, 2nd Ed. (CRC Press 1993), p.22.